Brain, Behavior, & Immunity - Health 41 (2024) 100848

Contents lists available at ScienceDirect

Brain, Behavior, & Immunity - Health

journal homepage: www.editorialmanager.com/bbih/default.aspx

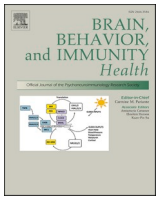

Chronic nasal inflammation early in life induces transient and long-term dysbiosis of gut microbiota in mice

Sanae Hasegawa-Ishii [a,*], Suzuho Komaki [a], Hinami Asano [a], Ryuichi Imai [a], Takako Osaki [b]

[a] Pathology Research Team, Faculty of Health Sciences, Kyorin University, 5-4-1 Shimorenjaku, Mitaka-shi, Tokyo, 181-8612, Japan
[b] Department of Infectious Diseases, Kyorin University School of Medicine, 6-20-2 Shinkawa, Mitaka, Tokyo, 181-8611, Japan

ARTICLE INFO

Keywords:
Suckling period
Dysbiosis
Nasal inflammation
Gut microbiota
Sex difference
Intranasal administration

ABSTRACT

The gut microbiota begins to colonize the host body following birth, develops during the suckling period and changes to the adult type after weaning. The early gut microbiota during the suckling period is thought to have profound effects on the host physiology throughout life but it is still unclear whether early dysbiosis is retained lifelong. Our previous study indicated that chronic nasal inflammation induces dysbiosis of gut microbiota in adult mice. In the present study, we addressed the question as to whether early exposure to chronic nasal inflammation induces dysbiosis, and if so, whether the dysbiosis is retained until adulthood and the sex differences in this effect. Male and female mice received repeated intranasal administration of lipopolysaccharide (LPS) or saline twice a week from P7 to P24 and were weaned at P24. The cecal contents were obtained for 16S rRNA analysis at 2 time points: at 4 weeks (wks), just after weaning, and at maturation to adulthood at 10 wks. The body weight did not differ between saline- and LPS-treated mice till around weaning, suggesting that the mothers' milk was given similarly to all mice. At 4 wks, the beta diversity was significantly different between saline- and LPS-treated male and female mice and the composition of the gut microbiota changed in LPS-treated mice. The abundance of phylum Bacteroidota tended to decrease and that of Firmicutes increased in LPS-treated male mice, while the abundance of Deferribacterota increased in LPS-treated female mice. At 10 wks, the beta diversity was not different between saline- and LPS-treated mice, but the abundance of family Lachnospiraceae significantly decreased in LPS-treated male and female mice by LEfSe analysis. Together, chronic nasal inflammation early in life caused transient and long-term dysbiosis of gut microbiota, which may contribute to the onset and progress of metabolic and neuropsychiatric disorders.

1. Introduction

The microbiota resides on all mucosal surfaces of the host body and the greatest amount and diversity colonizes the intestinal tract (Hill and Round, 2021). Gut bacteria cooperate with their hosts through a bidirectional network which consists of the immune, metabolic, and nervous systems (Rutsch et al., 2020; Morais et al., 2021). Gut microbiota begin to colonize the host body following birth and the initial colonizing bacteria are influenced by various factors including the delivery mode (vaginal vs Caesarean), feeding method (breast vs formula), maternal conditions (body weight, diet, and lifestyle risk factors during the gestation and breast-feeding period), as well as environmental factors (Milani et al., 2017; Tanaka and Nakayama, 2017; Dzidic et al., 2018; Kapourchali and Cresci, 2020). In infants born by vaginal delivery, the early gut bacteria resemble the mothers' vaginal bacteria dominated by *Lactobacillus*, *Prevotella*, and *Sneathia* spp., whereas those of infants born by Caesarean section resembles mothers' skin surface bacteria dominated by *Staphylococcus*, *Corynebacterium* and *Propionibacterium* spp. (Dominguez-Bello et al., 2010) After birth, the method of infant feeding is of high importance to the early gut microbiota. Breast-fed infants are more commonly colonized by aerobic organisms, while formula-fed infants are enriched with anaerobic organisms such as Bacteroides and Clostridium (Tanaka and Nakayama, 2017). When infants begin to eat solid food after weaning, the composition of the gut microbiota changes to the adult type, represented mainly by Bacteroidota and Firmicutes. This change is established around three years of age in humans (Yatsunenko et al., 2012; Valles et al., 2014).

Gut microbial disturbances in early life can potentially lead to adverse health outcomes later in life (Kapourchali and Cresci, 2020; Donald and Finlay, 2023). As an extreme example, maternal and infant

* Corresponding author.
E-mail address: sanae_ishii@ks.kyorin-u.ac.jp (S. Hasegawa-Ishii).

https://doi.org/10.1016/j.bbih.2024.100848
Received 8 January 2024; Received in revised form 30 July 2024; Accepted 17 August 2024

antibiotic exposure during gestation and breast-feeding period affects the maturation of the infant gut microbiota. The infants exposed to antibiotics show less diversity in their fecal bacterial communities and have lesser *Bifidobacterium* and unusual colonization with *Enterococcus* in the first week (Tanaka et al., 2009) and this dysbiosis remains until at least 2 years of age (Uzan-Yulzari et al., 2021). Although the detailed mechanisms are still unclear, antibiotic use and resulting dysbiosis early in life may increase the risk of a variety of diseases including obesity, (Trasande et al., 2013; Bailey et al., 2014) asthma (Zou et al., 2020), allergies (Metzler et al., 2019), inflammatory bowel disease (Ortqvist et al., 2019), type I diabetes (Candon et al., 2015), and even behavioral difficulties and symptoms of depression (Slykerman et al., 2017). As another example, maternal dietary factors, maternal stress, and gestational diabetes mellitus cause disruption in the fecal microbiota of not only mothers but also their infants (Kapourchali and Cresci, 2020; Anderson, 2020; Brawner et al., 2020), which may contribute to the onset of chronic metabolic and neuropsychiatric diseases later in life. However, it is still unknown whether dysbiosis during this early period is retained lifelong or returns to normal when the infants become adults.

In our previous study, we found that lipopolysaccharide (LPS)-induced chronic nasal inflammation causes dysbiosis of gut microbiota in adult mice (Mishima et al., 2021). After repeated intranasal LPS administration, male mice showed increased abundance of the phylum Bacteroidetes and decreased phylum Firmicutes. At the genus level, the abundance of *Bacteroides*, *Oscillospira*, *Parabacteroides* and *Prevotella* significantly increased, while that of *Allobaculum* and *Lactobacillus* significantly decreased. This pattern of dysbiosis with increased *Bacteroides* and decreased *Lactobacillus* has been previously reported to be associated with chronic stress in mice (Galley et al., 2014; Li et al., 2019) and major depressive patients (Jiang et al., 2015) in humans.

In the present study, we examined whether chronic nasal inflammation early in life would induce dysbiosis in infants, and if so, whether dysbiosis early in life would be retained throughout life. Male and female baby mice received intranasal administration of LPS or saline twice a week for 3 weeks during the suckling period (P7, P10, P14, P17, P21 and P24). The mice were weaned at P24, cecal contents were collected at 2 time points; just after weaning (at 4 weeks (wks)) and at maturation to adulthood (at 10 wks), and 16S rRNA analysis of cecal contents were performed.

2. Materials and Methods

2.1. Experimental procedure

C57BL/6J JmsSlc female mice that had been pregnant for 13 days (Sankyo lab, Tokyo, Japan) were purchased and housed in our facility. They gave birth to baby mice at day 19. At 7 days after the birth (P7), the baby mice were divided into 4 groups; saline male, LPS male, saline female and LPS female. P7 and P10 mice received 3 μL, P14 and P17 mice received 4 μL, and P21 and P24 mice received 5 μL of intranasal administration of either saline or LPS from *Escherichia coli* O55:B5 (1 mg/mL, Sigma). The volume of administration was determined to fill the nasal cavity so the volume increased as the baby mice grew up. Two mother mice, saline male, and LPS female baby mice were housed in one cage, while two mother mice, LPS male, and saline female baby mice were housed in another cage, in order to identify saline-treated and LPS-treated baby mice. Baby mice were exchanged between mother mice every week keeping the same sets (saline male and LPS female, or LPS male and saline female) to avoid maternal-dependent differences in the gut microbiota. Their body weight was measured once a week from P7 (saline male; n = 13 (P7 - P21), 12 (P28), 6 (P35, P63), 7 (P42 - P56), LPS male; n = 14 (P7 - P21), 12 (P28), 7 (P35 - P63), saline female; n = 19 (P7 - P21), 18 (P28), 13 (P35 - P56), 12 (P63) and LPS female; n = 21 (P7 - P21), 20 (P28), 14 (P35 - P63)). At P24, the mice were weaned, and male and female mice were housed separately, with saline- and LPS-treated mice in the same cage. All mice were served the same chow (CE-2, Sankyo Lab Service). Cecal contents were collected at 4 wks (P27 - 28) (saline male; n = 8, LPS male; n = 10, saline female; n = 10, and LPS female; n = 11) or 10 wks (saline male; n = 10, LPS male; n = 12, saline female; n = 10, and LPS female; n = 10). These samples were analyzed by 16S rRNA analysis (Fig. 1). The mortality rate after LPS nasal administration was zero. All protocols were approved by, and all methods were performed in accordance with the guidelines of the Institutional Animal Care and Use Committee of the Kyorin University Faculty of Health Sciences (Protocol 'I17-09-02-05'). In addition, this study was carried out in compliance with the ARRIVE guidelines.

2.2. Histological analysis

At 4 wks or 10 wks, mice were anesthetized with ketamine (100 mg/kg body weight) and xylazine (10 mg/kg) and transcardially perfused with phosphate buffered saline (PBS) and 4% paraformaldehyde in PBS as the fixation solution for 7 min (8 mL/min). The heads were further fixed in the same fixative overnight. Then the lower jaw and upper teeth were removed, and remaining skull and brain were placed in decalcification solution (2-times diluted K-CX, Falma, Tokyo, Japan) for 6 h at room temperature for decalcification, and then washed floating in water for more than 6 h. The skull and brain were cryoprotected with 20% sucrose at room temperature overnight embedded in OCT compound (Sakura Finetek, Torrance, CA, USA) and frozen in 100% ethanol cooled with dry ice. Frozen blocks were stored at −80 °C until use.

Olfactory mucosa was coronally cut into 16 μm slices using a cryostat, mounted on slide glasses, dried, and stored at −30 °C until use. The sections were rehydrated with TBST (Tris-HCl and 100 mmol/L with 0.1% Tween 20). Sections were immersed in Methanol with 0.3% hydrogen peroxide solution for 10 min, washed with TBST, and blocked with blocking buffer (5% normal donkey serum in TBST) at room temperature for 1 h. Then sections were incubated with primary antibodies (rat anti-Ly6G (1:200, AduoiGen, Liestal, Switzerland), F4/80 (1:200, Abcam, Cambridge, MA, USA) and goat anti-IL-1β (1:200, Abcam) antibodies) diluted in blocking buffer overnight. Sections were incubated with secondary antibody (ImmPress anti-rat IgG or anti-goat IgG, Vector Laboratories, Burlingame, CA, USA) at room temperature for 1 h, and stained with ImmPACT DAB (Vector Laboratories). Nuclei were counter stained with Carrazzi's hematoxylin for 1 min. Slices were cleared and coverslipped with HSR (Sysmex, Kobe, Japan). Sections were observed with an Eclipse Ci-L microscope equipped with a digital camera control unit (DS-Fi3/NIS-Elements; Nikon, Tokyo, Japan).

2.3. Collection of cecal contents

At 4 wks or 10 wks, mice were anesthetized with ketamine (100 mg/kg body weight) and xylazine (10 mg/kg). The abdomen was opened and the cecal contents were freshly collected, weighed and snap frozen with liquid nitrogen.

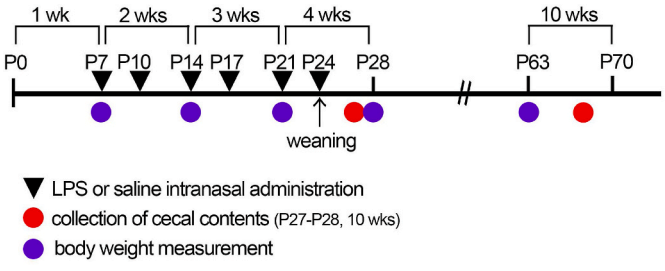

Fig. 1. Experimental protocol. Male and female baby mice received intranasal administration of saline or LPS at P7, P10, P14, P17, P21 and P24 and were weaned at P24. Cecal contents were collected at 4 wks (P27-28) and at 10 wks and used for 16S rRNA analysis. Body weight was measured once a week from P7 throughout the experiment. For histological analysis, mice were fixed by perfusion at 4 wks and 10 wks.

2.4. 16SrRNA analyses

Bacterial genomic DNA was extracted from cecal contents using Genomic DNA from stool samples (Macherey-Nagel GmbH & Co. KG, Germany). Each DNA specimen was amplified with universal primers targeting the 16S rRNA V3-V4 region Forward Primer (5′-TCGTCGGCAGCGTCAGATGTGTATAAGAGACAGCCTACGGGNGGCWGCAG) Reverse Primer (5′GTCTCGTGGGCTCGGAGATGTGTATAAGAGACAGGACTACHVGGGTATCTAATCC), with tag region. The amplicons were purified according to Irumina 16S Metagenomics Kit manufacturer directions (Illumina, San Diego, CA, USA) (Caporaso et al., 2012) and prepared for the sequencing library by using the Nextera XT index Kit according to the application manual. The sequencing runs were performed on an Illumina MiSeq (Illumina).

2.5. Bioinformatics

The 16S rRNA gene sequence data generated by the MiSeq sequencer (Illumina) were processed using the quantitative insights into microbial ecology 2 (QIIME October 2, 2019) pipeline (Bolyen et al., 2019). Raw sequence data were demultiplexed and quality filtered using the q2-demux plugin followed by denoising with DADA2 (Callahan et al., 2016). Taxonomy was assigned to ASVs using the q2-feature-classifier (Bokulich et al., 2018) classify-sklearn naïve Bayes taxonomy classifier against SILVA 138.1.

Within-community diversity (α-diversity) was calculated using QIIME2. An α-rarefaction was generated using a Chao 1, Shannon, Simpson, Simpson-e, evenness, faith and observed otus at each sampling depth. An even depth of ~17,400 sequences per sample was used for the calculation of richness and diversity indices.

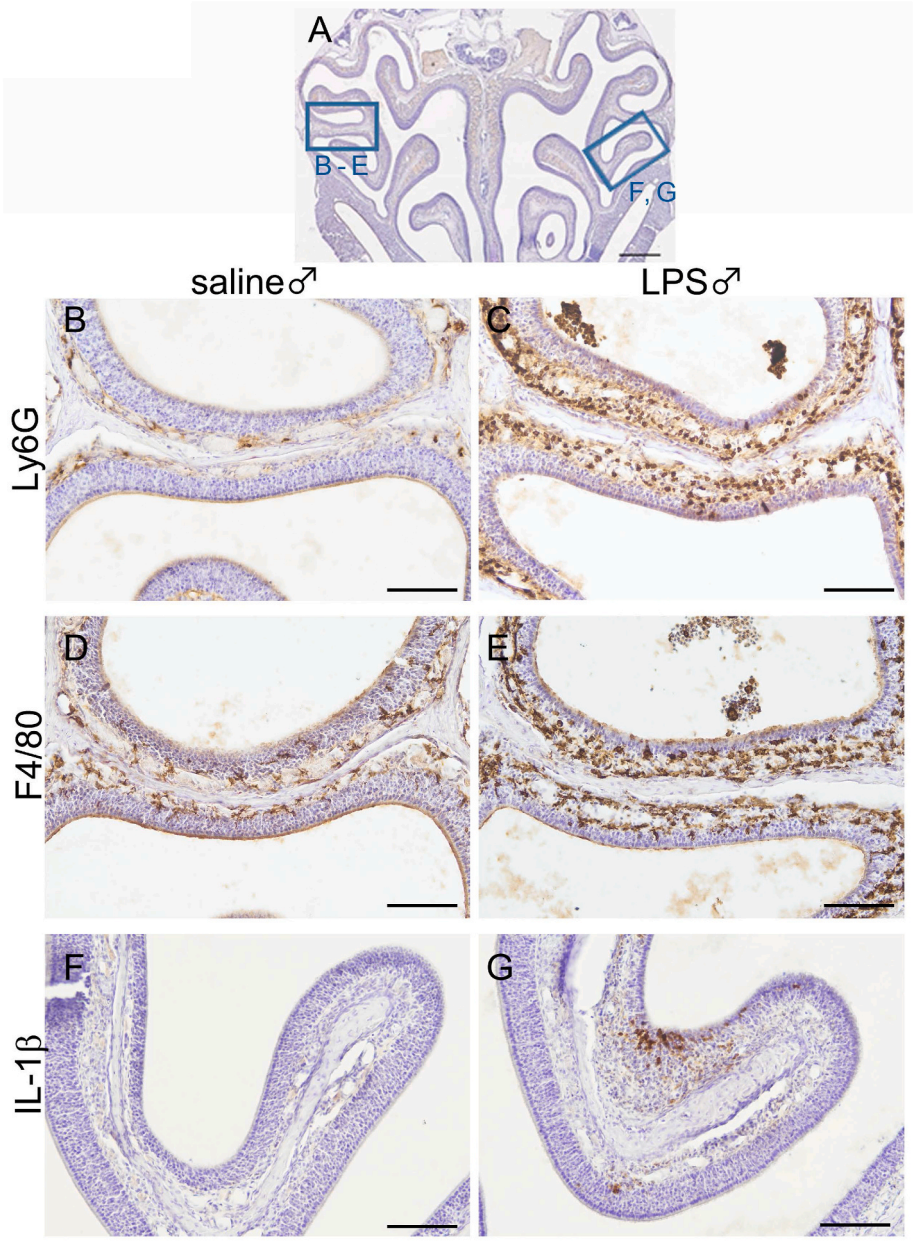

Fig. 2. Immunohistochemical staining of olfactory mucosa at 4 wks. A. Representative coronal section of the olfactory mucosa. Rectangles in the second turbinate are shown as magnified views in B-E or F and G. Many Ly6G-positive and F4/80-positive cells infiltrated the olfactory mucosa in LPS-treated mice (C and E) compared to saline-treated mice (B and D). IL-1β was expressed in some regions of the olfactory mucosa in LPS-treated mice (G) but not in saline-treated mice (F). Scale bars, 500 μm in A and 100 μm in B-G.

To compare microbial composition between samples, β-diversity was measured by calculating the Bray Curtis distances using QIIME2 default scripts. Principal coordinate analysis (PCoA) was applied to the resulting distance matrices to generate two-dimensional plots. A LEfSe approach was used to identify bacterial taxa that were significantly differentially abundant between each treatment group (Segata et al., 2011). Only taxa with a >2 log 10 LDA score were considered significantly enriched at a p value < 0.05.

2.6. Statistics

Changes in the body weight were compared statistically by 2 way-analysis of variance (ANOVA) (treatment: saline or LPS x time: P7, P14, P21, P28, P35, P42, P49, P56 and P63) followed by Tukey's HSD post hoc test. The thickness of the olfactory epithelium (OE) and the components of the bacteria at phylum level were also compared by 2-way ANOVA (treatment: saline or LPS x sex: male or female) followed by Tukey's HSD post hoc tests. Statistica software (Dell Software, Round Rock, TX) was used for multiple comparisons. A $p < 0.05$ represented a significant difference. Values are reported as means ± SEM.

3. Results

3.1. Nasal inflammation

First, we confirmed nasal inflammation using immunohistochemistry of the tissue sections of the olfactory mucosa (OM) (Fig. 2A). Ly-6G-positive and F4/80-positive immune cells increased in number in the OM and nasal cavity in LPS-treated male and female mice at 4 wks (Fig. 2C and E), while a smaller number of these cells were found in the lamina propria in saline-treated control (Fig. 2B and D). The expression of IL-1β was found in some specific regions of the OM after repeated intranasal LPS administration at 4 wks (Fig. 2G), but no IL-1β expression was detected in the saline-treated control (Fig. 2F).

The number of Ly6G-positive and F4/80-positive cells in the OM decreased in LPS-treated male and female mice at 10 wks compared to those at 4 wks, although the number of these cells was still higher compared to saline-treated control at 10 wks (Fig. 3A–D). The expression of IL-1β mostly subsided but was still found in some regions of the OM in LPS-treated mice at 10 wks (Fig. 3E and F). The thickness of the OE at the region shown in Fig. 3A–D was 46.3 ± 4.1 μm and 23.6 ± 0.8 μm in saline- and LPS-treated male mice, respectively. The OE thickness was significantly thinner in LPS-treated than in saline-treated male mice at 10 wks (Fig. 3B and D). Similarly, the thickness of OE was thinner in LPS-treated than in saline-treated female mice (41.2 ± 2.3 μm in saline-

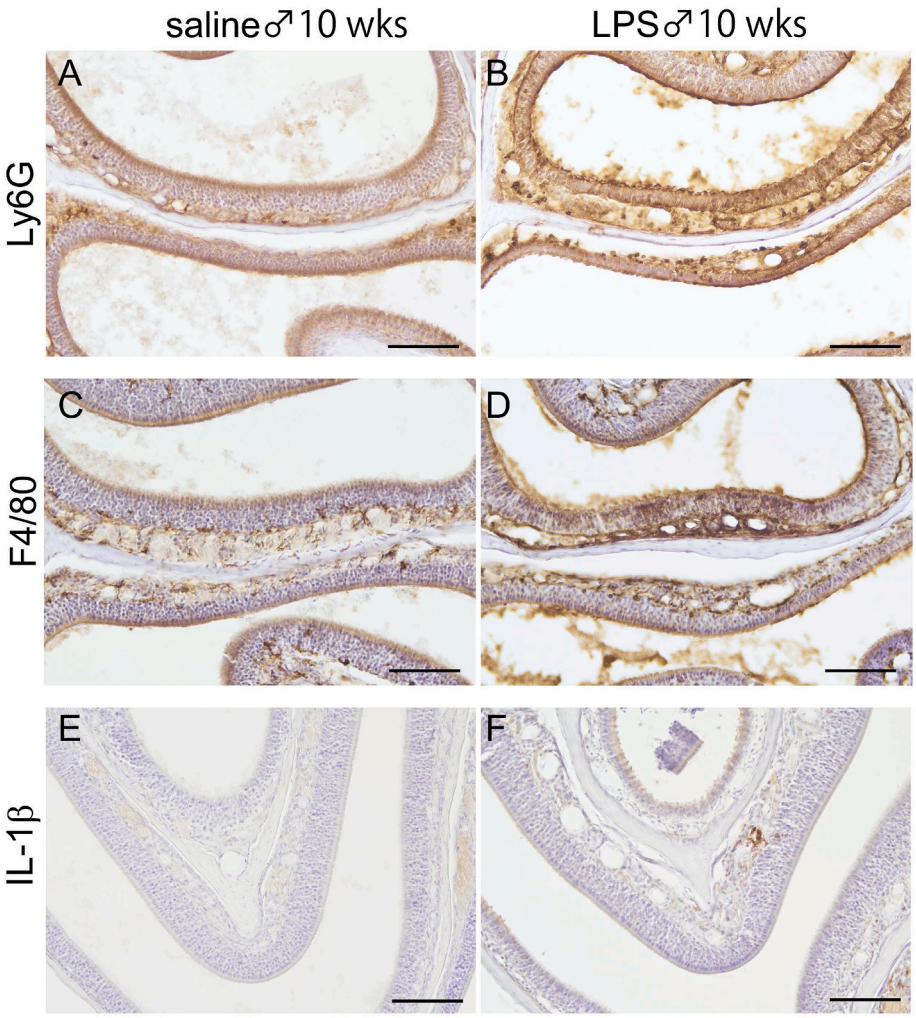

Fig. 3. Immunohistochemical staining of the olfactory mucosa at 10 wks. The number of Ly6G-positive and F4/80-positive cells in the olfactory mucosa decreased in LPS-treated mice at 10 wks (B and D) compared to those at 4 wks (Fig. 2C and E) but were still higher compared to saline-treated mice at 10 wks (A and C). IL-1β was still expressed in a few regions in the olfactory mucosa in LPS-treated mice at 10 wks (F), but not in saline-treated mice (E). Scale bars, 100 μm.

treated and 25.4 ± 1.0 μm in LPS-treated mice). These results suggest that nasal inflammation mostly, but not completely, subsided by 10 weeks of age (Fig. 3).

3.2. Growth curve of body weight

During the period of intranasal administration which was from P7 to P24 in the suckling period, the body weight increased similarly in saline- and LPS-treated mice. After weaning at P24, the body weight became transiently lower in LPS-treated male mice at P28 and tended to be lower at P35 compared to saline-treated male mice. The body weight, however, did not significantly differ later than P35 (Fig. 4). In female mice, the body weight was not significantly different between LPS- and saline-treated mice throughout the experiment (Fig. 4).

3.3. Comparison of gut microbiota between saline- and LPS-treated mice

3.3.1. Gut microbiota from cecal contents of 4-week-old mice

First, we compared the gut microbiota from cecal contents at 4 wks, when mice were just weaned after repeated intranasal administration. There were no significant differences in the alpha diversity between saline- and LPS-treated male or female mice. However, a significant difference was found in the beta diversity based on the analyses of Perm ANOVA between saline- and LPS-treated mice both in male and female mice by using the Bray-Curtis and Jaccard distance indices (q-values <0.1) (Fig. 5A). The beta diversity also showed sex differences between male and female mice. The same results were obtained in more than 2 separate experiments.

To compare the abundances among the 4 groups (saline male, LPS male, saline female and LPS female) at the phylum level, 2-way ANOVA (treatment x sex) was performed. The abundance of Firmicutes was higher and that of Bacteroidota tended to be lower ($p = 0.06$) in LPS-treated male mice, while that of Deferribacterota was higher in LPS-treated female mice, compared to saline-treated male or female mice, respectively (Fig. 5B). The ratio of Firmicutes to Bacteroidota (F/B value) was 1.42, 1.86, 1.65 and 1.79 in saline male, LPS male, saline female and LPS female mice, respectively, resulting in the tendency of higher F/B value ($p = 0.05$) in LPS-treated male mice compared to saline-treated male mice.

To compare the abundance of taxa between saline- and LPS-treated mice in detail, we performed LEfSe analysis and showed an LDA score that was more than 2 in male and female mice, separately (Fig. 5C and D). In male mice, class Clostridia in the phylum Firmicutes was higher in LPS-treated mice (red in Fig. 5C). In the class Clostridia, family Oscillospiraceae, genera *Oscillibacter*, *Peptococcus*, *Paludicola*, *Tuzzerella*, *Anaerotruncus*, and *Butyricicoccaceae* UCG_009 increased in abundance (red in Fig. 5C). Genus *Bilophila* was not in the class Clostridia but increased in LPS-treated male mice. In contrast, mainly 3 groups of bacteria were lower in LPS-treated male mice (green in Fig. 5C); phylum Bacteroidota, class Bacteroidia and order Bacteroidales; class Coriobacteria, order Coriobacteriales, family Eggerthellaceae, genus *Enterorhabdus;* phylum Proteobacteria, class Gammaproteobacteria, order Burkholderiales, family Sutterellaceae, genus *Parasutterella*. In the class Clostridia, order Monoglobales, family Monoglobaceae, genus *Monoglobus* and *Ruminococcaceae_Eubacterium_siraeum* group and *Oscillospiraceae* NK4A214 group were lower in LPS-treated male mice. In female mice, the abundances of phylum Deferribacterota, class Deferribacteres, order Deferribacterales, family Deferribacteraceae, and genus *Mucispirillum*; order Clostridia_vadinBB60 group; order Eubacteriales, family Anaerofustaceae, and genus *Aaerofustis*; family Ruminococcaceae, and genus *Faecalibaculum*, and genus *Tyzzerella*, *Lachnospiraceae_FCS020* group, and *Erysipelotrichaceae_unclassfied* were higher, while those of genera *Peptococcus* and *Turicibacter* were lower in LPS-treated female mice (Fig. 5D).

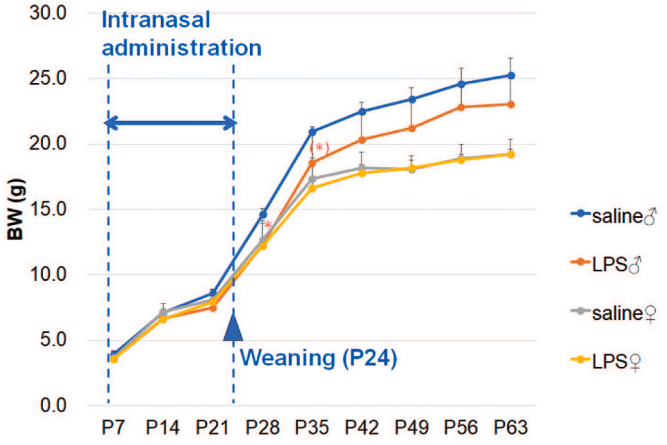

Fig. 4. Growth curve of body weight. Body weight increased with development similarly in saline- and LPS-treated male and female mice during the intranasal administration period (P7-P24). After weaning, body weight dropped significantly and tended to be lower at P28 and P35 in LPS-treated male mice but was not significantly different later than P35. In female mice, body weight was not significantly different throughout the experiments.

3.3.2. Gut microbiota from cecal contents of 10-week-old mice

Next, we analyzed gut microbiota from the cecal contents of 10-week-old mice that had received intranasal administration of saline or LPS during the suckling period. They showed no significant differences in the alpha or beta diversities between saline- and LPS-treated mice in either males or females (Fig. 6A). There was, however, a significant sex difference in the beta diversity by Bray Curtis and Jaccard distance between male and female mice.

Two way-ANOVA indicated that there were no significant differences at the phylum level between saline- and LPS-treated male mice, while the abundance of Desulfobacterota was significantly higher in LPS-treated female mice compared to that in saline-treated female mice (Fig. 6B). F/B value was 1.67, 1.65, 2.00 and 1.78 in saline male, LPS male, saline female and LPS female, respectively and there was no significant difference between saline- and LPS-treated mice. The abundance of phylum Bacteroidota tended to be higher in saline-treated male mice compared to that in saline-treated female mice, resulting in the tendency of a lower F/B value in male mice.

LEfSe analysis indicated that the class Clostridia was lower in LPS-treated male mice compared to saline-treated male mice (green in Fig. 6C). In the class Clostridia, order Lachnospirales, family Lachonospiraceae, and genus *Lachonospiraceae* NK4A136, and Clostridia_vadinBB60 group were lower and order Christensenellales, family Christensenellaceae, and *Oscillospiraceae* NK4A214 group were higher in LPS-treated male mice. In female mice, phylum Desulfobacterota, class Desulfovibrionia, order Desulfovibrionales, family Desulfovibrionaceae, and genus *Desulfovibrio* and genus *Alloprevotella* were higher, while order Lachonospirales, family Lachonospiraceae, and genus *Lachonospiraceae* UCG_006 were lower in LPS-treated female mice (Fig. 6D).

4. Discussion

In the present study, we examined the effects of chronic nasal inflammation early in life (P7-P24) on the components of the gut microbiota at 2 time points; just after weaning (at 4 wks), and at maturation to adulthood (at 10 wks). The baby mice were naturally born from healthy mothers and were taken care of by them during the suckling period. In addition, they shared the same mother mice (see Materials and Methods) to avoid maternal-dependent differences in gut microbiota. Moreover, we confirmed that the body weight of the baby mice increased similarly till around weaning, suggesting that they took on a similar amount of the mothers' milk in all groups. Thus, the external factors that can influence the formation of early gut microbiota were

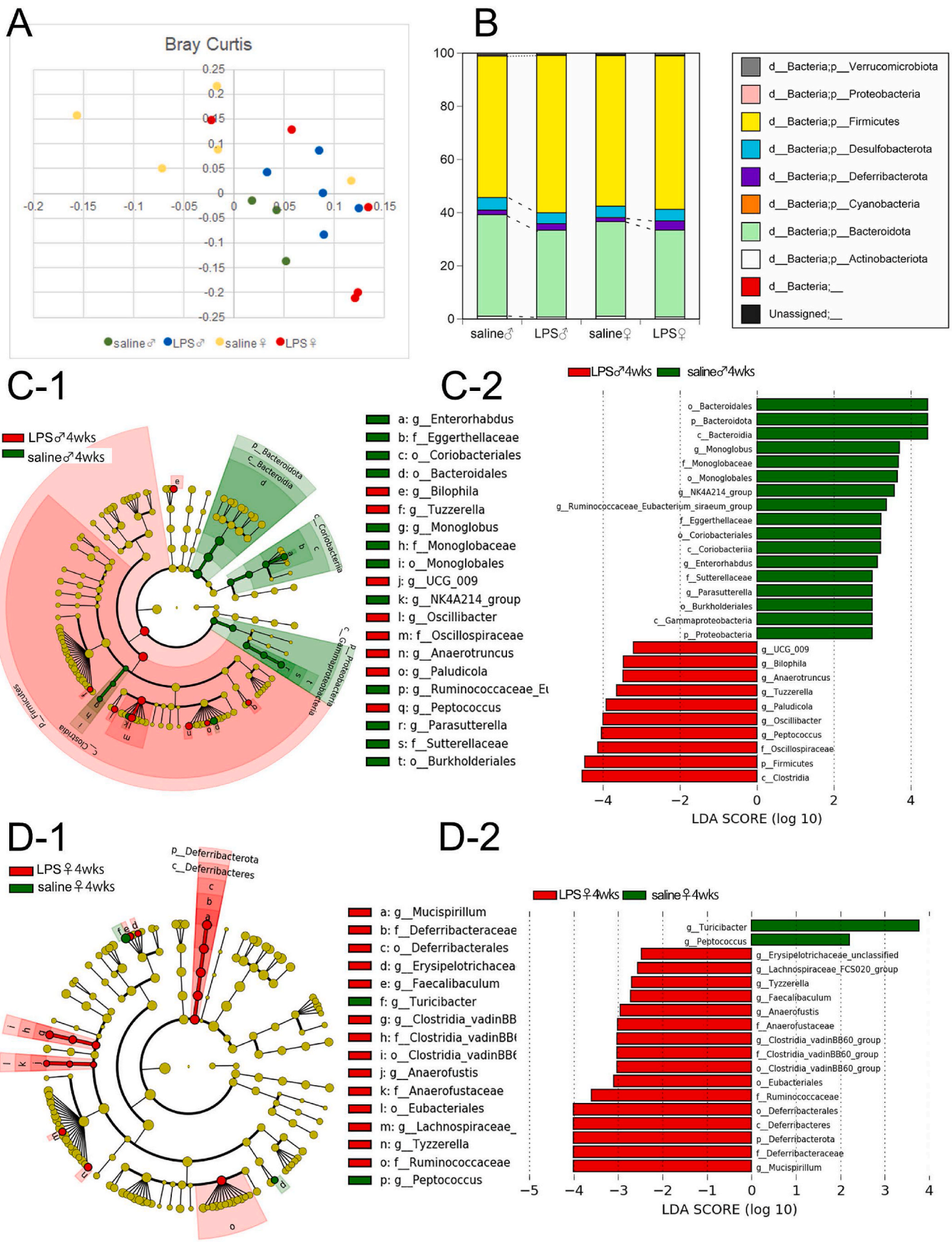

(caption on next page)

Fig. 5. Analysis of microbiota from cecal contents at 4 wks. A. Principle component analysis (PCA) based on Bray Curtis dissimilarities amongst all sample sets. Dots of different colors indicate samples collected from different groups. PC1: first principal coordinate, percent variation 20.56%; PC2: second principal coordinate, percent variation 12.24%. B. Phylum level of analysis of gut microbiota. C. LEfSe analysis of gut microbiota of male mice. C-1. Cladogram of the linear discriminant analysis (LDA) effect size (LEfSe) analysis shows the bacteria whose ratio is significantly different between saline- and LPS-treated male mice (Red, higher ratio in LPS-treated mice; green, higher ratio in saline-treated mice). C-2. Taxa significant from LEfSe (LDA score >2.0). D. LEfSe analysis of gut microbiota of female mice. D-1. Cladogram of the LEfSe analysis shows the bacteria whose ratio is significantly different between saline- and LPS-treated female mice (Red, higher ratio in LPS-treated mice; green, higher ratio in saline-treated mice). D-2. Taxa significant from LEfSe (LDA score >2.0). (For interpretation of the references to color in this figure legend, the reader is referred to the Web version of this article.)

similar in all the baby mice in this experiment. Nevertheless, the component of the gut microbiota in the cecal contents differed between saline- and LPS-treated mice at 4 wks and differed by sex. After weaning, saline- and LPS-treated mice were co-housed to avoid cage-dependent differences in gut microbiota. The difference in the beta diversity of the gut microbiota between saline- and LPS-treated mice at 4 wks did not appear at 10 wks and the gut microbiota in LPS-treated mice tended to that of the saline-treated mice. However, LEfSe analysis indicated that the abundance of some bacteria still differed in LPS-treated mice at 10 wks, probably due to impaired development of gut microbiota.

1. Nasal inflammation-induced transient dysbiosis of the gut microbiota in male mice

After repeated LPS intranasal administration during the suckling period, the abundance of phylum Bacteroidota tended to decrease and Firmicutes significantly increased, resulting in the tendency of an increased F/B value in the cecal contents of LPS-treated male mice at 4 wks. The phyla Bacteroidota and Firmicutes are 2 dominant bacteria in the gut and account for about 90% of the total gut bacteria in mice. Thus, the change in the F/B value is indicative of dysbiosis.

According to the LEfSe analysis, genera *Bilophila*, *Anaerotruncus*, *Tuzzerella,* and *Oscillibacter* increased in the cecal contents in LPS-treated male mice at 4 wks. These bacteria are known as 'harmful' or 'inflammation-associated' bacteria. Genus *Bilophila* is commonly regarded as a pathobiont and is known to increase in abundance in patients with active pancolitis compared to healthy subjects (Maldonado-Arriaga et al., 2021). In addition, the abundance of genus *Bilophila* is higher in patients with major depressive disorder (MDD) and those in remission of MDD (Caso et al., 2021). Genus *Anaerotruncus* has been known to have pro-inflammatory properties and has been identified as a potential biomarker for colorectal cancer recurrence and patient prognosis (Huo et al., 2022). Moreover, it has been shown that high fat diet and fatigue is associated with increase in abundance of *Anaerotruncus* (Liu et al., 2023). A high fat diet also increases the abundance of *Oscillibacter* in fecal microbiota, which is correlated with increased permeability in the proximal colon (Lam et al., 2012). *Oscillibacter* has also been reported to be associated with trimethylamino oxide, a risk factor for cardiovascular and cerebrovascular disease (Yin et al., 2015). The abundance of *Tuzzerella* increases with intake of high fat/high sugar diet (Pessoa et al., 2023). In contrast, genera *Monoglobus* and *Parasutterella* decreased in the cecal contents in LPS-treated male mice. They are recently known to decrease in subjects with sleep deprivation, in which significantly higher inflammation and dysregulation of the circadian rhythms were exhibited (Yang et al., 2023). In the present study, we showed that intranasal LPS administration changed the abundance of these harmful and inflammation-associated bacteria in the cecal contents of male mice. One possible route connecting the nasal inflammation to the gut dysbiosis may be systemic inflammation. To address the possibility that nasal inflammation induced systemic inflammation, we tried ELISA and mass spectrometry analyses of the serum. However, the results did not indicate any increase in the pro- or anti-inflammatory cytokines, such as IL-1β, TNFα, IL-6 or IL-10 nor an increase in the amount of anti-LPS antibody or total IgG in serum after repeated LPS intranasal administration (Data not shown). Another possibility could be that some of the nasal bacteria or intranasally administered LPS may be swallowed and directly enter and act on the gastrointestinal tract. This has been shown previously in a study in which orally injected *Porphyromonas gingivalis* accessed the gut and perturbed the flora (Arimatsu et al., 2014). As such, when LPS is intranasally administered, potentially altered nasal bacteria and/or LPS itself may be swallowed and reach the intestine to affect the gut microbiota. In addition, intranasally administered LPS may activate nasopharynx associated lymphoid tissue, which affects the mucosal immune system (Kiyono and Fukuyama, 2004).

In the previous study, LPS-induced chronic nasal inflammation caused dysbiosis in adult male mice with decreased phylum Firmicutes and increased Bacteroidetes (Mishima et al., 2021), the opposite results from the present study. In general, the ratio of Firmicutes to Bacteroidota increases during development in humans (Mariat et al., 2009). In accordance with the fact, our results showed that the abundance of phylum Bacteroidota was higher and Firmicutes lower in 4-week-old mice compared to adult mice. Thus, phylum Bacteroidota in 4-week-old mice and Firmicutes in adults may be more susceptible to alteration due to their higher ratios.

2. Nasal inflammation-induced transient dysbiosis of the gut microbiota in female mice

In female mice, the major bacteria such as the phyla Bacteroidota or Firmicutes did not change in the abundance after chronic nasal inflammation, but a milder dysbiosis occurred. Genus *Mucispirillum* in the phylum Deferribacterota increased in abundance. This is a harmful bacterium positively associated with increased plasma level of LPS and is assumed to be a microbial marker of colitis (Rooks et al., 2014). Members of the *Erysipelotrichaceae* family have a high abundance in the intestinal tract of mammals and increased in abundance in LPS-treated female mice in the present study. Genus *Erysipelotrchaceae* has been reported to increase in high fat or western diet mice (Fleissner et al., 2010) and patients with chronic HIV infection in addition to pro-inflammatory cytokine expression (Dinh et al., 2015). While these 'harmful' bacteria increased in the LPS-treated female mice in the present study, conversely the 'beneficial bacteria' such as *Lachnospiraceae* FCS020 group, *Faecalibaculum*, and *Ruminococcaceae*, which produce short chain fatty acids (SCFA) and provide beneficial effects to the host, concomitantly increased in the cecal contents, suggesting that these bacteria contribute to avoiding perturbation of gut microbiota in female mice.

3. Long-term effect of intranasal LPS administration on the gut microbiota

After weaning, mice begin to take solid food by themselves instead of their mothers' milk, which induces significant changes in the gut microbiota. Comparing the gut microbiota between 4 wks and 10 wks in the saline-treated control male mice, phyla Desulfobacterota decreased and the phyla Firmicutes increased in adult male mice (Supplementary Figure 1A). In the phylum Firmicutes, families Lachnospiraceae, Oscillospiraceae, and Butyricicoccaceae increased in abundance, which is the normal maturation of gut microbiota in male mice. However, male mice that had received intranasal LPS administration during the suckling period had lower abundance of genus *Lachonospirace* NK4A136 in family Lachnospiraceae at 10 wks (Fig. 6C). This result may show that early intranasal LPS administration interfered with normal maturation of the gut microbiota.

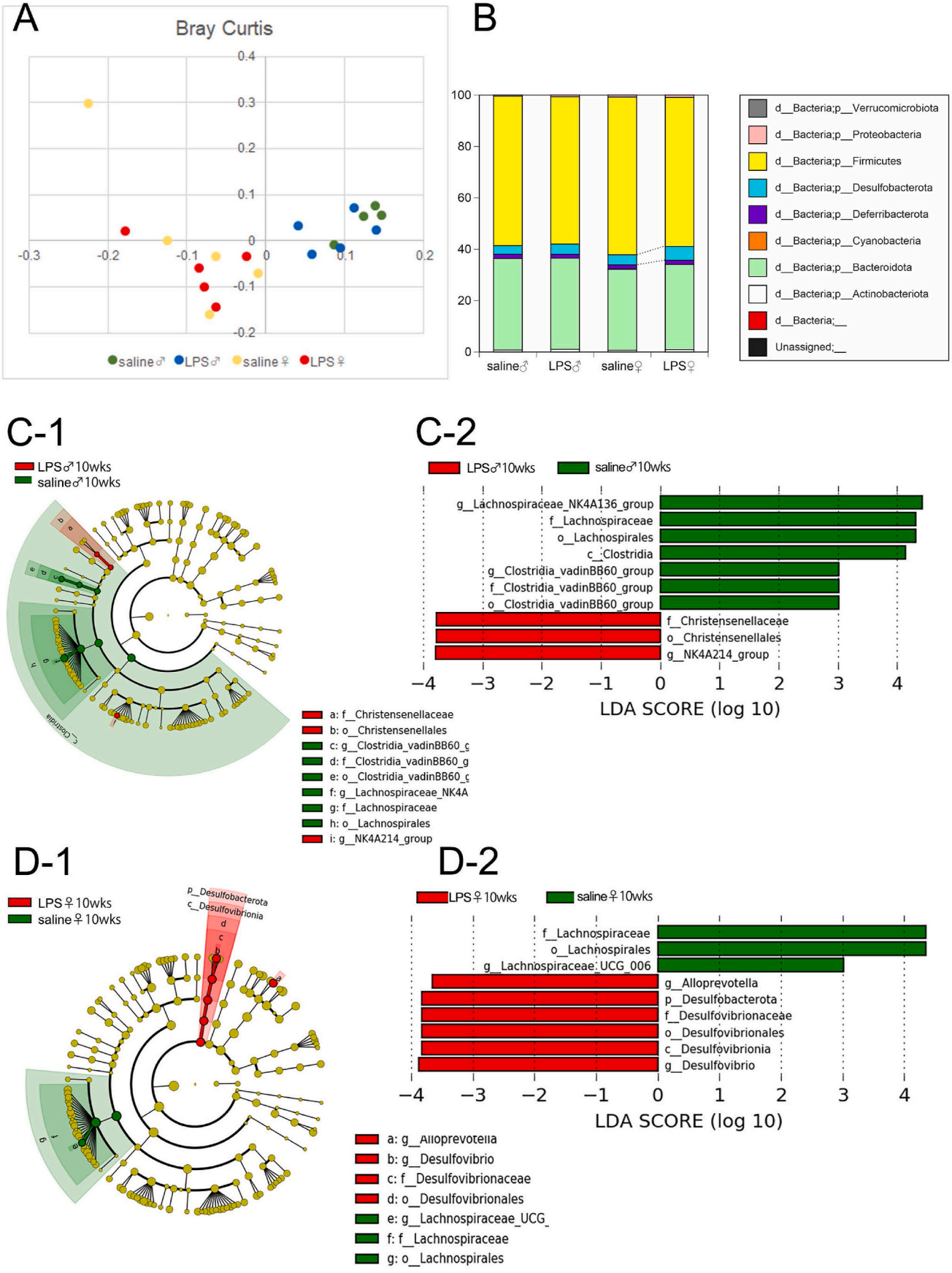

(caption on next page)

Fig. 6. Analysis of microbiota from cecal contents at 10 wks. A. PCA based on Jaccard dissimilarities amongst all sample sets. Dots of different colors indicate samples collected from different groups. PC1: first principal coordinate, percent variation 18.17%; PC2: second principal coordinate, percent variation 13.73%. B. Phylum level of analysis of gut microbiota. C. LEfSe analysis of gut microbiota of male mice. C-1. Cladogram of the LEfSe analysis shows the bacteria whose ratio is significantly different between saline- and LPS-treated male mice (Red, higher ratio in LPS-treated mice; green, higher ratio in saline-treated mice). C-2. Taxa significant from LEfSe (LDA score >2.0). D. LEfSe analysis of gut microbiota of female mice. D-1. Cladogram of the LEfSe analysis shows the bacteria whose ratio is significantly different between saline- and LPS-treated female mice (Red, higher ratio in LPS-treated mice; green, higher ratio in saline-treated mice). D-2. Taxa significant from LEfSe (LDA score >2.0). (For interpretation of the references to color in this figure legend, the reader is referred to the Web version of this article.)

Among the family Lachnospiraceae, the genus *Lachnospiraceae* NK4A136 is a butyrate-producing bacterium and has been known to maintain gut barrier integrity. Butyrate is one of the main SCFAs produced by bacteria and is important in maintaining intestinal health due to its ability to enhance epithelial barrier integrity and inhibit inflammation (Ma et al., 2020). Decreased level of the genus *Lachnospiraceae* NK4A136 has been found in mice with obesity (Ma et al., 2020), periodontitis (Li et al., 2021), acute kidney inflammation (Zou et al., 2022), experimental colitis (Huang et al., 2022; Thipart et al., 2023), and depression (Cheng et al., 2018). In a rat model of hydrocortisone-induced depression, the relative abundance of *Lachnospiraceae* NK4A136 was significantly decreased, which correlated to increased quinoline content, a neurotoxic metabolite in the tryptophan-kynurenine metabolic pathway (Cheng et al., 2018). Thus, decreased *Lachnospiraceae* NK4A136 found in the LPS-treated male mice may contribute to host metabolic and neuropsychiatric disorders.

In female mice, intranasal LPS administration during the suckling period increased the phylum Desulfobacterota, genus *Desulfovibrio* and decreased the family Lachnospiraceae, and genus *Lachnospiraceae* UCG-006 at 10 wks. The family Desulfovibrionaceae is a Gram-negative bacterium producing LPS and the genus *Desulfovibrio* is known as a harmful and pathogenic bacterium. These bacteria could induce macrophages to secrete more TNF-α, resulting in aggravation of intestinal damage (Zhou et al., 2021). The *Lachnospiraceae* UCG-006 group is an anti-inflammatory bacterium positively related to cecal SCFA levels and negatively related to serum IL-6 and hepatic AST and ALT levels in LPS-treated mice (Guo et al., 2021). In addition, the disturbance of genus *Lachnospiraceae* UCG-006 may contribute to the onset of depressive-like behaviors via regulating phosphatidylcholine and phosphatidylethanolamine metabolism (Xu et al., 2024). Thus, in both male and female mice, intranasal LPS administration early in life had a long-term effect on the gut microbiota.

4 Significance of this study

Nasal inflammation is easily caused by air pollution and various pathogens in the environment after birth. In the fetal period, when pathogens residing in the external genitalia of a mother access the amniotic fluid, the fetus may swallow the infected amniotic fluid into the oral and nasal cavity (Adams Waldorf and McAdams, 2013), potentially resulting in nasal inflammation in the fetus. Maternal and neonatal immune activation leads to neuropsychiatric disorders such as autism spectral disorders and schizophrenia (Estes and McAllister, 2016), although the detailed mechanisms are still being examined. Antibiotics are commonly used to the mother in the clinical setting, which influence the microbiota of infants through maternal dysbiosis of vaginal, skin, breast milk, and gut microbiota (Kapourchali and Cresci, 2020). The present study indicates that infant dysbiosis has long-term effects on the gut microbiota even when the infant develops toward adulthood, which may contribute to the onset and progress of metabolic and neuropsychiatric diseases.

5. Conclusion

Chronic nasal inflammation early in life caused transient and long-term dysbiosis, likely due to interference with the normal maturation of gut microbiota. Male mice suffered a more severe effect of nasal inflammation on the cecal gut microbiota than female mice. The mechanisms underlying the dysbiosis of gut microbiota caused by nasal inflammation and the effects of decrease in the abundance of family Lachnospiraceae on the host health remain to be studied.

CRediT authorship contribution statement

Sanae Hasegawa-Ishii: Writing – review & editing, Writing – original draft, Project administration, Methodology, Investigation, Funding acquisition, Formal analysis, Data curation, Conceptualization. **Suzuho Komaki:** Investigation, Data curation. **Hinami Asano:** Investigation, Data curation. **Ryuichi Imai:** Investigation. **Takako Osaki:** Writing – original draft, Supervision, Methodology, Funding acquisition, Conceptualization.

Declaration of competing interest

None.

Data availability

Data will be made available on request.

Acknowledgement

This study was supported by the Grant-in-Aid for Scientific Research KAKENHI 21K07280 (to S. H-I.), 22K07164 (to T. O.), and 24K11176 (to S. H-I. and T. O.), a grant from Mishima Kaiun Memorial Foundation (to S. H–I.) and a collaborative research grant from Kyorin University (to S. H-I.). We thank Dr. Kentaro Oka for his contribution to microbiome analysis, and Mr. Shota Aoyama, Ms. Nami Sugai, Ms. Nao Suzuki for their contribution to animal experiments.

Appendix A. Supplementary data

Supplementary data to this article can be found online at https://doi.org/10.1016/j.bbih.2024.100848.

References

Adams Waldorf, K.M., McAdams, R.M., 2013. Influence of infection during pregnancy on fetal development. Reproduction 146, R151–R162. https://doi.org/10.1530/REP-13-0232.

Anderson, G., 2020. Pathoetiology and pathophysiology of borderline personality: role of prenatal factors, gut microbiome, mu- and kappa-opioid receptors in amygdala-PFC interactions. Prog. Neuro-Psychopharmacol. Biol. Psychiatry 98, 109782. https://doi.org/10.1016/j.pnpbp.2019.109782.

Arimatsu, K., et al., 2014. Oral pathobiont induces systemic inflammation and metabolic changes associated with alteration of gut microbiota. Sci. Rep. 4, 4828. https://doi.org/10.1038/srep04828.

Bailey, L.C., et al., 2014. Association of antibiotics in infancy with early childhood obesity. JAMA Pediatr. 168, 1063–1069. https://doi.org/10.1001/jamapediatrics.2014.1539.

Bokulich, N.A., et al., 2018. Optimizing taxonomic classification of marker-gene amplicon sequences with QIIME 2's q2-feature-classifier plugin. Microbiome 6, 90. https://doi.org/10.1186/s40168-018-0470-z.

Bolyen, E., et al., 2019. Author Correction: reproducible, interactive, scalable and extensible microbiome data science using QIIME 2. Nat. Biotechnol. 37, 1091. https://doi.org/10.1038/s41587-019-0252-6.

Brawner, K.M., Yeramilli, V.A., Kennedy, B.A., Patel, R.K., Martin, C.A., 2020. Prenatal stress increases IgA coating of offspring microbiota and exacerbates necrotizing enterocolitis-like injury in a sex-dependent manner. Brain Behav. Immun. 89, 291–299. https://doi.org/10.1016/j.bbi.2020.07.008.

Callahan, B.J., et al., 2016. DADA2: high-resolution sample inference from Illumina amplicon data. Nat. Methods 13, 581–583. https://doi.org/10.1038/nmeth.3869.

Candon, S., et al., 2015. Antibiotics in early life alter the gut microbiome and increase disease incidence in a spontaneous mouse model of autoimmune insulin-dependent diabetes. PLoS One 10, e0125448. https://doi.org/10.1371/journal.pone.0125448.
Caporaso, J.G., et al., 2012. Ultra-high-throughput microbial community analysis on the Illumina HiSeq and MiSeq platforms. ISME J. 6, 1621–1624. https://doi.org/10.1038/ismej.2012.8.
Caso, J.R., et al., 2021. Gut microbiota, innate immune pathways, and inflammatory control mechanisms in patients with major depressive disorder. Transl. Psychiatry 11, 645. https://doi.org/10.1038/s41398-021-01755-3.
Cheng, D., et al., 2018. Tiansi liquid modulates gut microbiota composition and Tryptophan(-)Kynurenine metabolism in rats with hydrocortisone-induced depression. Molecules 23. https://doi.org/10.3390/molecules23112832.
Dinh, D.M., et al., 2015. Intestinal microbiota, microbial translocation, and systemic inflammation in chronic HIV infection. J. Infect. Dis. 211, 19–27. https://doi.org/10.1093/infdis/jiu409.
Dominguez-Bello, M.G., et al., 2010. Delivery mode shapes the acquisition and structure of the initial microbiota across multiple body habitats in newborns. Proc. Natl. Acad. Sci. U. S. A. 107, 11971–11975. https://doi.org/10.1073/pnas.1002601107.
Donald, K., Finlay, B.B., 2023. Early-life interactions between the microbiota and immune system: impact on immune system development and atopic disease. Nat. Rev. Immunol. 23, 735–748. https://doi.org/10.1038/s41577-023-00874-w.
Dzidic, M., Boix-Amoros, A., Selma-Royo, M., Mira, A., Collado, M.C., 2018. Gut microbiota and mucosal immunity in the neonate. Med. Sci. 6 https://doi.org/10.3390/medsci6030056.
Estes, M.L., McAllister, A.K., 2016. Maternal immune activation: implications for neuropsychiatric disorders. Science 353, 772–777. https://doi.org/10.1126/science.aag3194.
Fleissner, C.K., et al., 2010. Absence of intestinal microbiota does not protect mice from diet-induced obesity. Br. J. Nutr. 104, 919–929. https://doi.org/10.1017/S0007114510001303.
Galley, J.D., et al., 2014. Exposure to a social stressor disrupts the community structure of the colonic mucosa-associated microbiota. BMC Microbiol. 14, 189. https://doi.org/10.1186/1471-2180-14-189.
Guo, W., et al., 2021. Protective effects of microbiome-derived inosine on lipopolysaccharide-induced acute liver damage and inflammation in mice via mediating the TLR4/NF-kappaB pathway. J. Agric. Food Chem. 69, 7619–7628. https://doi.org/10.1021/acs.jafc.1c01781.
Hill, J.H., Round, J.L., 2021. SnapShot: microbiota effects on host physiology. Cell 184, 2796–2796 e2791. https://doi.org/10.1016/j.cell.2021.04.026.
Huang, J.Q., et al., 2022. Chimonanthus nitens oliv. Leaf granule ameliorates DSS-induced acute colitis through treg cell improvement, oxidative stress reduction, and gut microflora modulation. Front. Cell. Infect. Microbiol. 12, 907813 https://doi.org/10.3389/fcimb.2022.907813.
Huo, R.X., et al., 2022. Gut mucosal microbiota profiles linked to colorectal cancer recurrence. World J. Gastroenterol. 28, 1946–1964. https://doi.org/10.3748/wjg.v28.i18.1946.
Jiang, H., et al., 2015. Altered fecal microbiota composition in patients with major depressive disorder. Brain Behav. Immun. 48, 186–194. https://doi.org/10.1016/j.bbi.2015.03.016.
Kapourchali, F.R., Cresci, G.A.M., 2020. Early-life gut microbiome-the importance of maternal and infant factors in its establishment. Nutr. Clin. Pract. 35, 386–405. https://doi.org/10.1002/ncp.10490.
Kiyono, H., Fukuyama, S., 2004. NALT- versus Peyer's-patch-mediated mucosal immunity. Nat. Rev. Immunol. 4, 699–710. https://doi.org/10.1038/nri1439.
Lam, Y.Y., et al., 2012. Increased gut permeability and microbiota change associate with mesenteric fat inflammation and metabolic dysfunction in diet-induced obese mice. PLoS One 7, e34233. https://doi.org/10.1371/journal.pone.0034233.
Li, N., et al., 2019. Fecal microbiota transplantation from chronic unpredictable mild stress mice donors affects anxiety-like and depression-like behavior in recipient mice via the gut microbiota-inflammation-brain axis. Stress 22, 592–602. https://doi.org/10.1080/10253890.2019.1617267.
Li, L., et al., 2021. Gut microbiota may mediate the influence of periodontitis on prediabetes. J. Dent. Res. 100, 1387–1396. https://doi.org/10.1177/00220345211009449.
Liu, J., Qiao, B., Cai, Y., Tan, Z., Deng, N., 2023. Diarrhea accompanies intestinal inflammation and intestinal mucosal microbiota dysbiosis during fatigue combined with a high-fat diet. BMC Microbiol. 23, 151. https://doi.org/10.1186/s12866-023-02896-9.
Ma, L., et al., 2020. Spermidine improves gut barrier integrity and gut microbiota function in diet-induced obese mice. Gut Microb. 12, 1–19. https://doi.org/10.1080/19490976.2020.1832857.
Maldonado-Arriaga, B., et al., 2021. Gut dysbiosis and clinical phases of pancolitis in patients with ulcerative colitis. Microbiologyopen 10, e1181. https://doi.org/10.1002/mbo3.1181.
Mariat, D., et al., 2009. The Firmicutes/Bacteroidetes ratio of the human microbiota changes with age. BMC Microbiol. 9, 123. https://doi.org/10.1186/1471-2180-9-123.
Metzler, S., et al., 2019. Association between antibiotic treatment during pregnancy and infancy and the development of allergic diseases. Pediatr. Allergy Immunol. 30, 423–433. https://doi.org/10.1111/pai.13039.
Milani, C., et al., 2017. The first microbial colonizers of the human gut: composition, activities, and health implications of the infant gut microbiota. Microbiol. Mol. Biol. Rev. 81 https://doi.org/10.1128/MMBR.00036-17.
Mishima, Y., Osaki, T., Shimada, A., Kamiya, S., Hasegawa-Ishii, S., 2021. Sex-dependent differences in the gut microbiota following chronic nasal inflammation in adult mice. Sci. Rep. 11, 4640. https://doi.org/10.1038/s41598-021-83896-5.
Morais, L.H., Schreiber, H.L.t., Mazmanian, S.K., 2021. The gut microbiota-brain axis in behaviour and brain disorders. Nat. Rev. Microbiol. 19, 241–255. https://doi.org/10.1038/s41579-020-00460-0.
Ortqvist, A.K., Lundholm, C., Halfvarson, J., Ludvigsson, J.F., Almqvist, C., 2019. Fetal and early life antibiotics exposure and very early onset inflammatory bowel disease: a population-based study. Gut 68, 218–225. https://doi.org/10.1136/gutjnl-2017-314352.
Pessoa, J., Belew, G.D., Barroso, C., Egas, C., Jones, J.G., 2023. The gut microbiome responds progressively to fat and/or sugar-rich diets and is differentially modified by dietary fat and sugar. Nutrients 15. https://doi.org/10.3390/nu15092097.
Rooks, M.G., et al., 2014. Gut microbiome composition and function in experimental colitis during active disease and treatment-induced remission. ISME J. 8, 1403–1417. https://doi.org/10.1038/ismej.2014.3.
Rutsch, A., Kantsjo, J.B., Ronchi, F., 2020. The gut-brain Axis: how microbiota and host inflammasome influence brain physiology and pathology. Front. Immunol. 11, 604179 https://doi.org/10.3389/fimmu.2020.604179.
Segata, N., et al., 2011. Metagenomic biomarker discovery and explanation. Genome Biol. 12, R60. https://doi.org/10.1186/gb-2011-12-6-r60.
Slykerman, R.F., et al., 2017. Antibiotics in the first year of life and subsequent neurocognitive outcomes. Acta Paediatr. 106, 87–94. https://doi.org/10.1111/apa.13613.
Tanaka, M., Nakayama, J., 2017. Development of the gut microbiota in infancy and its impact on health in later life. Allergol. Int. 66, 515–522. https://doi.org/10.1016/j.alit.2017.07.010.
Tanaka, S., et al., 2009. Influence of antibiotic exposure in the early postnatal period on the development of intestinal microbiota. FEMS Immunol. Med. Microbiol. 56, 80–87. https://doi.org/10.1111/j.1574-695X.2009.00553.x.
Thipart, K., et al., 2023. Dark-purple rice extract modulates gut microbiota composition in acetic acid- and indomethacin-induced inflammatory bowel disease in rats. Int. Microbiol. 26, 423–434. https://doi.org/10.1007/s10123-022-00309-x.
Trasande, L., et al., 2013. Infant antibiotic exposures and early-life body mass. Int. J. Obes. 37, 16–23. https://doi.org/10.1038/ijo.2012.132.
Uzan-Yulzari, A., et al., 2021. Neonatal antibiotic exposure impairs child growth during the first six years of life by perturbing intestinal microbial colonization. Nat. Commun. 12, 443. https://doi.org/10.1038/s41467-020-20495-4.
Valles, Y., et al., 2014. Microbial succession in the gut: directional trends of taxonomic and functional change in a birth cohort of Spanish infants. PLoS Genet. 10, e1004406 https://doi.org/10.1371/journal.pgen.1004406.
Xu, K., et al., 2024. Oral D-ribose causes depressive-like behavior by altering glycerophospholipid metabolism via the gut-brain axis. Commun. Biol. 7, 69. https://doi.org/10.1038/s42003-023-05759-1.
Yang, D.F., et al., 2023. Acute sleep deprivation exacerbates systemic inflammation and psychiatry disorders through gut microbiota dysbiosis and disruption of circadian rhythms. Microbiol. Res. 268, 127292 https://doi.org/10.1016/j.micres.2022.127292.
Yatsunenko, T., et al., 2012. Human gut microbiome viewed across age and geography. Nature 486, 222–227. https://doi.org/10.1038/nature11053.
Yin, J., et al., 2015. Dysbiosis of gut microbiota with reduced trimethylamine-N-oxide level in patients with large-artery atherosclerotic stroke or transient ischemic attack. J. Am. Heart Assoc. 4 https://doi.org/10.1161/JAHA.115.002699.
Zhou, J., et al., 2021. P16 (I NK 4a) deletion ameliorates damage of intestinal epithelial barrier and microbial dysbiosis in a stress-induced premature senescence model of bmi-1 deficiency. Front. Cell Dev. Biol. 9, 671564 https://doi.org/10.3389/fcell.2021.671564.
Zou, Z., Liu, W., Huang, C., Sun, C., Zhang, J., 2020. First-Year antibiotics exposure in relation to childhood asthma, allergies, and airway illnesses. Int. J. Environ. Res. Publ. Health 17. https://doi.org/10.3390/ijerph17165700.
Zou, Y.T., et al., 2022. Gut microbiota mediates the protective effects of traditional Chinese medicine formula qiong-yu-gao against cisplatin-induced acute kidney injury. Microbiol. Spectr. 10, e0075922 https://doi.org/10.1128/spectrum.00759-22.